Structural characterization of interpenetrating network formation of high acyl gellan and maltodextrin gels

Kanyuck, K. M.; Norton-Welch, A. B.; Mills, T. B.; Norton, I. T.

DOI:
10.1016/j.foodhyd.2020.106295

Document Version
Peer reviewed version

Citation for published version (Harvard):
Kanyuck, KM, Norton-Welch, AB, Mills, TB & Norton, IT 2021, 'Structural characterization of interpenetrating network formation of high acyl gellan and maltodextrin gels', *Food Hydrocolloids*, vol. 112, 106295. https://doi.org/10.1016/j.foodhyd.2020.106295

Structural Characterization of Interpenetrating Network Formation of High Acyl Gellan and Maltodextrin Gels

K. M. Kanyuck*, A. B. Norton-Welch, T. B. Mills, I. T. Norton

School of Chemical Engineering, University of Birmingham, Edgbaston, Birmingham, B15 2TT, UK

*Contact information for the corresponding author: Kelsey Kanyuck. Tel: +44 121 414 5364 Email: KXK720@student.bham.ac.uk

Abstract

A mixed-gel of high acyl (HA) gellan gum and maltodextrin (MD) (potato DE2) demonstrated a range of physical properties with a proposed interpenetrating network. Mixed hydrocolloid gels allow for the development of novel properties that neither polymer alone could create allowing unique functionality in textures or controlled release. The aim of this work was to identify the type of network formation by examining material properties and the contribution from of each polymer. Material properties of quiescently set composite gels were characterized through bulk fracture, small deformation rheology, DSC, and microscopy. A continuous shift in fracture strain and modulus were created through mixed gels of the soft and flexible HA gellan with the firm and brittle MD. By adding MD (from 0 to 40%) at a constant 0.5% gellan, the gel true strain at fracture decreased from 0.50 to 0.18 while the Young's Modulus increased from 3 to 1780 kPa. No indication of phase separation or chemical complexation was measured. Analysis of the time-dependant MD contribution and composite material properties hypothesized a gelation mechanism in which HA gellan forms a network first and MD aggregates within the pores without phase separation. MD dominated the small deformation rheology while HA gellan appeared to dominate the fracture point. Material properties were indicative of the type of structural organization in the HA gellan MD mixed gel network.

Keywords. Maltodextrin; High Acyl Gellan Gum; Interpenetrating Network; Mixed Hydrocolloids; Gel Fracture

1. Introduction:

Mixed biopolymer gel systems have become popular to achieve a wider and more controllable range of properties than any single gelling system. Applications in the food industry include creation of novel textures, mimicking of traditional foods with improved nutritional profiles (low and no-fat), and controlled release functionality. The key to understanding the properties of composite gels lies in a microstructural understanding of the gel network formation (Norton and Frith, 2001). Mixed gel networks are divided into three idealized types: phase separated, interpenetrating (IPN), and coupled (Morris, 1986; Kasapis, 1995; Norton et al., 2014). Interactions between two polymers may either be segregative or associative based on the enthalpy of interaction of between similar versus dissimilar polymers (Morris, 2009). A phase separated network originates from segregative interactions and is often observed as a water-in-water dispersion in which one polymer forms droplets within a continuous network of the second polymer (Morris 2009, Norton 2014). Both IPN and coupled are types of associative interactions between polymers. For an IPN gel, both polymers form networks spanning the gel in one phase and without direct interaction of the polymers (Kasapis, 1995; Norton et al., 2014). A coupled network additionally involves a chemical association between the two types of polymer, and this type has only been observed in a few systems (Morris, 1995; Kasapis, 1995; Morris, 2009). A key distinction between these types for polymers that gel by forming aggregates, which may appear as phase separated, is whether phase separation occurs prior to gelation (true phase separated by segregative interactions) or the gelation mechanism simply leads to regions rich in one polymer (micro-phase separated or interpenetrating) (Clark et al., 1999; Djabourov et al., 2013). Phase separated system are common because frequently the enthalpic contribution from like-to-like polymer interactions outweighs the association of dissimilar polymers and small entropic contribution of staying mixed (Kasapis et al., 1993c; Clark, 1996; Morris, 2009). Interpenetrating networks occur when the enthalpic contribution of separation is low (such as with a charged and an uncharged polymer). This work will examine the network formation between high acyl (HA) gellan and maltodextrin. The first section will examine the type and mechanism of network formation and the second will examine contributions of each polymer to composite modulus and fracture behaviour.

Maltodextrin (MD) gels are formed by dense aggregate regions which form strong brittle gels at high concentrations (Schierbaum et al., 1992; Chronakis, 1998; Loret et al., 2004; Kanyuck et al., 2019). This polymer is a carbohydrate created through the hydrolysis of starch into shorter chains (Chronakis, 1998). A low dextrose equivalent (DE) MD has a lower degree of hydrolysis, and it is the longer chains of these MDs which exhibit gelling abilities. Gelation occurs by aggregation of double helix chains of polymer strands and the presence of sufficient long stands that are able to connect multiple aggregate regions (Reuther et al., 1984; Radosta and Schierbaum, 1990). For the DE 2 potato MD used, critical gelling concentration are reported between 15 and 20% by weight (Kasapis et al., 1993b; Loret et al., 2004; Kanyuck et al., 2019).

High acyl (HA) gellan gum forms a soft and flexible gel with a high strain to fracture caused by a fibrous gel network (Sanderson et al., 1988; Funami et al., 2008). Gelation occurs through double helix formation of individual chains (Chandrasekaran et al., 1992), and helices are connected by branching and end-to-end associations (Morris et al., 1999; Noda et al., 2008; Funami et al., 2008). Unlike many hydrocolloids, there is limited helix aggregation due to the steric hindrance of the acetyl groups (Noda et al., 2008; Funami et al., 2008). The microbial fermented hydrocolloid is an acidic carbohydrate comprising of a four-sugar repeated unit with 0.9 glycerate and 0.4 acetate groups on the first sugar unit and one carboxyl group on the second unit (Kasapis et al., 1999; Sworn, 2009). The more commonly studied variant low acyl (LA) gellan gum has the same carboxyl groups

but the deacetylation process removed most of the bulky acyl groups, thus changing the gel structure and material properties (Morris et al., 2012).

MD has been studied in mixed gelling systems previously, and most often for applications in fat reduction due to the creaminess mimicking abilities of MDs (Chronakis, 1998). Most literature has proposed phase separated mixed gels between a low DE MD and gelatin (Kasapis et al., 1993a; Lorén and Hermansson, 2000), low methoxy pectin (Picout et al., 2000), agarose (Loret et al., 2006), iota carrageenan (Wang and Ziegler, 2009), milk protein (Chronakis et al., 1996), locust bean gum, gum acacia, and high salt carboxymethyl cellulose (Annable et al., 1994). For charged polymers, phase separation was either not observed with high methoxy pectin (Evageliou et al., 2000) or was only observed at sufficient levels of added salts with carboxymethyl cellulose (Annable et al., 1994). One researcher has suggested the presence of an IPN formed with MD in combination with low acyl (LA) gellan (Clark et al., 1999). Experimentation with HA gellan is limited, although the non-gelling polymers of chitosan fibers (Liu et al., 2013) and soybean fiber (Chen et al., 2020) have been proposed to arrange within the pores without phase separation. No published work has examined the mixed gel of HA gellan and MD, and there is only limited knowledge of the interactions between HA gellan with other hydrocolloids.

The large disparity between the material properties of MD and HA gellan gum allowed a rheological analysis of the microstructure contribution of each polymer to the mixed gel. This work proposes the structural organization of the mixed gel is reflective in the physical and chemical properties of the composite. Materials properties, microscopy, DSC, and modelling of composite gels will be used to characterize the mixed gel of MD with HA gellan gum. Contributions of each polymer to specific material properties will also be discussed to examine the structural influence of individual gel networks.

2. Material and Methods:

2.1. Materials and Gel Preparation

HA gellan gum (KELCOGEL LT100 lot # 5B1259A) was obtained from CP Kelco (UK). MD (Paselli SA-2) was purchased from Avebe (Netherlands) produced from potato with a dextrose equivalent (DE) between 2.7 and 2.9 (Kasapis et al., 1993b; Manoj et al., 1996). The salt content of HA gellan was 19473 ppm potassium, 3615 ppm sodium, 2187 ppm calcium, and 29 ppm magnesium as measured by ICP-OES (Optima 8000 by PerkinElmer). The DE 10 MD (Paselli SA-10) was purchased from Avebe (Netherlands), the modified MD originated from waxy corn starch and was modified to increased branching and lower the molecular weight (Agenanova from Agrana, Austria), and the glucose was purchased from Sigma Aldrich (UK). DI water was purified with a reverse osmosis milli-Q water system.

Prior to mixing, each polymer was dispersed individually to ensure complete hydration. HA gellan was mixed into DI water at 90 °C and hydrated for 2 hours with stirring to reach a stock concentration between 4 and 5% (Cassanelli et al., 2018). MD was slowly dispersed in DI water at 95 °C and stirred for 4 hours to hydrate at stock concentrations ranging from 40% to 60% (Kanyuck et al., 2019). Glucose and the other MDs (DE 10 and modified) were prepared identically by fulling hydrating in heated water prior to mixing. Water loss was accounted for by replacing any lost mass to the sample during heating. Gels were prepared by mixing these heated stock solutions together with the required amount of heated DI water to achieve the range of concentrations utilized in this work. Hot solutions were stirred until homogenous (approximately 5 minutes) and quiescently set in plastic cylindrical molds (20 mm diameter) excluding the samples for DSC which were prepared in

specific vessels. Gels for time-dependent measurements were prepared from a single solution to produce five samples, and at each of the time points one sample was measured and destroyed.

2.2. Compression and Fracture of Gels

Bulk material properties were assessed by compression of gels with a squeeze-flow setup using a TA.XT.plus texture analyser (Stable Micro Systems, UK). Samples were prepared using a 20 mm diameter cylindrical mold and cut to a 20 mm height. Gels were compressed with a speed of 2 mm/s between parallel surfaces of a flat probe (40 mm diameter) and a stationary stage until fracture (up to a 90% reduction of the initial sample height). Further deformation was not possible with the instrument and would have resulted in gel material squeezing outside the geometry and loosing contact with the upper plate. From the instrumental measurement of force (F) and distance (ℓ), the Young's Modulus (E), true strain (ε_T), and true stress (σ_T) were calculated:

$$E = \sigma/\varepsilon \text{ from } \varepsilon = 0.01 \text{ to } \varepsilon = 0.05 \quad (1)$$

$$\varepsilon_T = \ln((\ell_0 + (\ell_0 - \ell) / \ell_0) \quad (2)$$

$$\sigma_T = (F/A_0) (1 + \varepsilon) \quad (3)$$

When 'ℓ_0' is the initial sample height and A_0 the initial contact area of 314 mm^2.

2.3. Differential Scanning Calorimetry

A µDSC3evo (Seteram Instrumentation, France) was used with a temperature range of 20 to 95 °C with a heating and cooling rate of 0.2 °C/min with 10 minute isothermal holds at each extreme. A second heating and cooling step was performed immediately following the first. Only the first heating and cooling are shown graphically but calculated enthalpies are reported for all steps. Integration and curve smoothing was preformed using CALISTO software (Seteram Instrumentation, France). Enthalpies were normalized to grams of total sample and curves were compiled after a manual linear baseline subtraction. Prior to data collection, gels were pre-melted in the DSC by heating and cooling at 1 °C/min from 20° to 95° C with a 10 minute hold at 95° to ensure a homogenous sample over the bottom of the vessel. For adequate measurement of the MD contribution to the gel, all samples were held at room temperature for 4 days prior to the reported DSC analysis (Kanyuck et al., 2019). Gels were added hot with a mass of 0.8 ± 0.1 g and a matching mass of DI water. Sample and reference cells had a volumetric capacity of ~ 0.9 mL and were sealed vessels of Hastelloy material.

2.4. Modelling by Polymer Blending Laws

The isostress and isostrain equations are often used to model physical properties of phase separated gel systems based on a composite of the individual polymers. Theory and models were adapted from E. R. Morris (1992). The equations predict the composite gel modulus (G_C), using the phase volume of HA gellan gum (ϕ_{HAG}) and MD (ϕ_{MD}) and calculated modulus at the effective concentration of HA gellan gum (G_{HAG}) and MD (G_{MD}):

$$\text{Isostrain } G_c = \phi_{HAG}G_{HAG} + \phi_{MD}G_{MD} \quad (4)$$

$$\text{Isostress } 1/G_c = \phi_{HAG}/G_{HAG} + \phi_{MD}/G_{MD} \quad (5)$$

Application of these models to biopolymer gels relied on several assumptions that required modification; no polymer volume, complete phase separation, and a mathematically model-able modulus (Morris, 1992). Firstly, the assumption of no polymer volume is invalid in this system with MD concentrations up to 40% (Manoj et al., 1996). To account for this, effective concentrations of

each polymer were expressed as polymer per water (w/w) ($Mass_{polymer}$ / $Mass_{water}$) to calculate the modulus. This modification allows consideration to the concentrating effect that a 30% MD solution would have on the effective HA gellan gum concentration through a reduction in the amount of water in the total mixture. For example, a 1% HA gellan gum with 30% MD would be calculated using the water amount of 69% and the effective concentration becomes 1.4%. Secondly, the concept of calculating phase volumes (ϕ) became difficult without observation of any separation so typical methods of measuring volume of each water phase were not applicable to this system. Relaxation rates ($1/T_2$) of single polymer gels and mixed gels were used to approximate the proportional water binding by shifts in the composite relaxation rates. Addition of 1% HA gellan caused a shift along the entire curve approximately equal to 10% MD, and thus a 1% HA gellan to 10% MD equivalence point was estimated (Supplement Figure 1). Previous effective concentration measurements for LA gellan and MD were modelled non-linearly but values were of a similar ratio (Clark et al., 1999). Variations above and below this ratio were tested in the models, but similar fits to the reported values were obtained. We acknowledge many assumptions were made from this simplification, and this value merely represents the closest possible approximation of a value we propose is meaningless in the mixture. Effective concentration models (Figures 4C and 4D) did not utilize the assumption of phase volumes. Concentration curves of individual polymers were used to estimate the contribution of each individual polymer. Polynomial equations from predictive models were written for calculations of modulus at any effective concentration (G_{HAG} and G_{MD}).

2.5 Scanning Electron Microscopy (SEM)

SEM measurements were acquired using a JEOL 6060LV (Tokyo, Japan). Samples were cut into 1.5 x 1.5 mm cubes and suspended 1 cm above liquid nitrogen for one minute and then immersed in liquid nitrogen for one minute. An aluminium sample stage and carbon tab were cooled via immersion in liquid nitrogen for one minute. Images were acquired using back scatter electrons (BSE), a low vacuum of 50 Pa, an accelerating voltage of 10 kV, and a 10 mm working distance.

2.6 Statistical Analysis

Figures show the average of at least three samples and error bars represent the standard deviation. Statistical lettering was used in Table 2 to distinguish statistically different ($p < 0.05$) samples after using an ANOVA and all pairwise comparison test with the Student-Newman-Keuls method (SigmaPlot 12.5). In reference to the discussion of Figure 8 and Table 1, the claim of “no change with time” was based on a comparison of means for each concentration of MD and a p-value of 0.01 to account for the number of pairwise comparisons.

3. Results and Discussion:

3.1 Network Characterization

Fracture mechanics, lack of continuous phase discontinuity, disagreement with phase-separated models, cumulative bond energies, and microscopy will be discussed to support the proposition of an interpenetrating network of HA gellan and MD. Above critical gelling concentrations of both polymers, a true IPN network was suggested and was consistent with the mechanism proposed for LA gellan and MD by Clark et al. (1999) whereby the MD aggregated within a porous gellan network without phase separation. Below the gelling concentration of MD (approximately 20%), a non-segregative gel was comprised of MD aggregates within a continuous HA gellan network.

3.1.1 Material Properties

Material properties of the gels were measured by compression of cylindrical shaped samples using a texture analyzer. The compression curves were measured as force over distance and converted to true stress and true strain using equations 1 and 2 (Section 2.2) with examples of representative curves in Figure 1. Arrows point out the fracture point for each sample. Strain at fracture, stress at fracture, and modulus were observably different by examining the shape of compression profiles between individual gels of MD and gellan (solid lines). MD alone at a concentration of 30% formed a firm gel with a large modulus and showed brittle fracture at 0.13 true strain (Figure 1). Conversely, the 1% HA gellan was soft and flexible with fracture only at 0.56 true strain. The composite gels resulted in intermediate strain at fracture and modulus (Figure 1). For the composite gels, only one fracture point was observed.

Fracture points of the composite material and the contribution of polymer concentrations are displayed in Figure 2. HA gellan gum was very flexible with high strains to fracture (0.49 to 0.59) while MD alone fractured at low strains (0.14-0.18). Mixtures showed fracture points varying between the two individual polymer values. A common indication of a phase separated gel is a large shift in behaviour (discontinuous) from switching between continuous phases (Norton and Firth, 2001). A phase separated system would be expected to show strain values determined by the continuous polymer (with some modification from the interface) and a large shift when the continuous phase changed (Norton and Frith, 2001). This was not observed and the incremental change in fracture strain of the composite gel (non-discontinuous) suggests there is not bulk phase separation. Increasing levels of MD also increased the Young's Modulus of the mixed gel (Figure 3). All samples of HA gellan without the inclusion of MD resulted in comparatively low moduli (2500 – 5000 Pa). The curve shapes of the Young's Modulus of mixed gel closely followed the MD curve (□) with a small increase from greater HA gellan concentrations (Figure 3). HA gellan had a much smaller modulus than MD, by one to two orders of magnitude, so the minimal contribution was not unexpected.

MD independently did not form a gel below 20%, and at 15% the solution was still pourable with visibly increased light scattering from chain aggregation (Kasapis et al., 1993b; Loret et al., 2004; Kanyuck et al., 2019). Below the gelling concentration, aggregates are proposed to be adding inhomogeneity to the HA gellan network as well as overall rigidity to the composite by acting as filler particles. The formation of aggregated regions of MD within a rearranged HA gellan network are consistent with the deswelling and "elongated configurations" proposed when co-gelling with LA gellan (Kasapis et al., 1999). Below the gelation point of MD, the decreased strain to failure is suggested to have originated from inhomogeneities in the HA gellan network created by the MD. For most food gels, the fracture point occurs when the applied force becomes greater than the cohesive bonds and the concentration of polymer does not actually effect the strain at fracture (Zhang et al., 2005).The failure point is expected to be characterized by the microstructure defects and energy dissipation mechanism, which initiate and propagate fracture respectively (Van Vliet and Walstra, 1995). Aggregation of MD into large dense regions within the HA gellan network is feasible to have created cracks or inhomogeneities. This aggregation is proposed to modify the loose HA gellan network into less flexible regions. These heterogeneities within the network act as cracks and focus the stresses to cause a more brittle fracture (Van Vliet and Walstra, 1995). Above the gelling concentration (20%) which coincides with the largest changes in strain, MD is proposed to reach a critical number of aggregates to form a second continuous network. Only at this point is the mixed gel network hypothesized to create two interpenetrating networks. Below the gelation point of MD (20%), MD appeared to act as a filler particle without formation of a secondary gel network. Bulky aggregates appeared to have sterically hindered compression by decreasing mobility of the HA gellan network in the mixed gel.

3.1.2. Microstructure Analysis

Theoretical models can be utilized to analyse the relationship between microstructure and function. Phase separated biopolymers have commonly been understood by modelling individual contributions to isostrain and isostress models by considering effective concentrations and assuming complete phase separation. A phase separated system is suggested when predicted values from these models are similar to the measured values, although minor deviation is always expected (Kasapis, 2008). Utilizing the models refined by Morris (1992), the equations were modelled for 0.5%, 1% and 1.5% HA gellan with increasing concentrations of MD (Figure 4). Even without phase separation, changes in effective concentrations of each polymer should be expected (Clark et al., 1999). All estimates have been modified to effective concentrations (considered a percentage of the water mass in the sample) to account for the high solid content of MD, comparable to the method of Manoj et al. (1996). True Isostrain and isostress predications are shown in Figure 4A, 4B, and 4C which takes into account the effective concentrations after an assumed phase separation of the polymers. Alternatively, Figure 4D, 4E, and 4F only adjusts the concentration based on the total water within a sample and assumes no liquid-liquid demixing. Both models utilize the in-series model (isostress) and the in-parallel (isostrain) models for the contribution of each polymer (equations 4 and 5). Other concentrations of HA gellan were also modelled and showed equivalent trends and quality of fit and thus are not included for redundancy.

The phase-separated models (Figure 4A-C) were not a good fit for the observed composite moduli. At most concentrations of MD (below 25%), the measured modulus was weaker than predicted. When liquid-liquid mixing occurs, higher effective concentrations of each polymer occur in both phases. In this system, no indication of phase separation by increases in modulus from higher effective concentrations was observed. Additionally, at higher MD concentrations neither phase-separating model could predict the measured composite modulus effectively. The prediction from the non-phase separating models (Figure 4D-F) were closer to the measured values. At low concentrations (0-10% MD), none of the models predict a deviation far from that of HA gellan alone and was consistent with measured values (Figure 4D-F). The rise in modulus with increasing MD was best accounted in the single phase isostrain model, which is consistent with the compositional theory of two networks spanning the length of the gel (Ross-Murphy, 1995). Similarity of models in Figure 4D-F to the measured values suggested a lack of phase separation which could be consistent with either an IPN or coupled network.

Glucose-based polymers of various sizes were substituted at equivalent concentrations with 1% HA gellan in an attempt to separate the aggregation (solid filler) and solvent quality effects of MD from the network effects. Material properties of these gels are summarized in Table 1. The DE 2 MD is the one used throughout this paper. The DE 10 MD is also from potato and further hydrolysed so that it can form aggregates but is unable to form a gel network. The modified MD (with increased branching) and glucose are unable to form aggregates or a gel network. Comparison of these three analogues to the DE 2 MD allowed for determination of the influence of network formation specifically. Changes in solvent quality or water of hydration (mimicked by glucose or the modified MD) only showed a small (less than 10%) change in composite modulus at fracture strain and highlighted the importance of DE 2 gelation on composite fracture and modulus (an increase of 6,000 %). The contribution of MD to the mixed gel originates in network structure formation beyond just a small influence from changes to the solvent. Fracture strain was only decreased with the DE 2 and DE 10 MDs (Table 1) which both form aggregates (Kasapis et al., 1993b).The DE 10 MD is able to form aggregates but is thought to not have enough long chains to gel, although the composite flexibility was still decreased. Aggregation of these MDs can also be seen in the time dependence (a

change in modulus over 14 days, which is discussed in section 3.2) while no effect was seen for the modified MD nor the glucose. In these mixed gels, aggregates appear to have created enough structural inhomogeneities in the HA gellan to increase brittleness of the composite gel. A network formation by the DE 2 MD was indicated by the increase large increase in modulus that not even the non-aggregating MD exhibited.

Table 1. Comparison of material properties of 1% HA gellan gels with 30% carbohydrate additives. Time dependence refers to a significant change ($p < 0.05$) in Young's Modulus or true strain at fracture over the period of 1 and 14 days.

Carbohydrate Type	**Young's Modulus (Pa)**	**Strain at Fracture**	**Stress at Fracture (kPa)**	**Time Dependence**
MD DE 2	235,707 ± 42,000	0.32 ± 0.01	122 ± 3	Yes
MD DE 10	3,300 ± 200	0.47 ± 0.01	25 ± 2	Yes
Modified MD (non-aggregating)	3,300 ± 250	0.57 ± 0.01	207 ± 16	No
Glucose	3,600 ± 90	0.57 ± 0.01	184 ± 11	No
No Additive (1.5%)	3,870 ± 82	0.58 ± 0.01	283 ± 29	No
No Additive (1.0%)	3,200 ± 100	0.56 ± 0.01	114 ± 18	No

Gel networks were further compared by differential scanning calorimetry (DSC) to check for associations between polymers indicative of a coupled network. Heat flow of gels melting (A) and cooling (B) are shown in Figure 5. The range of melting temperatures (between peak onset and offset) from both polymers was quite broad and has been attributed to low cooperation between aggregates (Morris et al., 1996; Mazen et al., 1999). Individually, the 1% HA gellan showed gelling and melting temperatures of 63 °C and 60 °C respectively (Figure 5) and was consistent with the small hysteresis usually reported because of the minimal aggregation of helices (Morris et al., 1996; Kasapis et al., 1999; Mazen et al., 1999; Morris et al., 2012). Heating curves for MD showed a broad breaking of the network during melting, but no observable bonds were measured during the cooling process (Figure 5B). Although unusual for most hydrocolloids, this is consistent with the long gelling time of multiple days for MD (Loret et al., 2004; Kanyuck et al., 2019). The slight upward movement of the MD curve approaching 25 °C could be from the beginning of detection of MD aggregation. There was indication that some bonds slowly reformed evidenced by the melting enthalpy of 27% of the original during the second heating cycle (Table 2).

Melting endotherms and enthalpy were additive without indication of increased enthalpy or bonds between polymers. Enthalpy values were not different than a pure summation of the two polymers (Table 2) and no new bonds were suggested by new peaks at different melting temperatures (Kasapis, 2008). The first melting cycle includes both MD aggregates and HA gellan gel helices melting as samples were held for 4 days prior to analysis. In cooling, only the HA gellan was observed to gel within the experimental timeframe (which is consistent with the proposed mechanism of slow MD gelation). A slight increase in gelling temperature between HA gellan with or without MD can be attributed to an increase in effective concentration of the HA gellan component. Due to the 20% MD in the formation, less water resulted in an effective concentration of 1.25% which was consistent with a melting temperature of 66 °C (Supplementary Figure 2). The enthalpy respective to gelation of the HA gellan was unchanged by the MD ($p>0.05$). Additive bond energies were consistent with an IPN or phase separated gel, and inconsistent with a coupled network. Preceding analysis has eliminated the phase separated model and jointly the results are only consistent with an IPN.

Table 2. Calculated enthalpy values (J/g) from DSC heating and cooling cycles based on grams of total sample. Values are reported as the average with one standard deviation for three replicates. Different letters indicate significantly different sample means.

	1st Cycle (4 day gelation)		2nd Cycle	
	Heating	Cooling	Heating	Cooling
HA Gellan (1%)	$0.13^{A} \pm 0.04$	$0.12^{A} \pm 0.04$	$0.10^{A} \pm 0.01$	$0.09^{A} \pm 0.01$
MD (20%)	$1.74^{D} \pm 0.09$	**	$0.47^{B} \pm 0.07$	**
Measured HA Gellan (1%) + MD (20%)	$1.92^{E} \pm 0.16$	$0.12^{A} \pm 0.01$	$0.59^{C} \pm 0.12$	$0.13^{A} \pm 0.01$
Summation of HA Gellan (1%) + MD (20%)	1.87	0.12	0.57	0.09

** peaks could not be resolved from baseline

Microscope images of a 30% MD gel and a mixed gel of 25% MD and 1% HA gellan are shown in Figure 6. Images were representative of the entire gel that was viewed and no signs of macroscopic phase separation were observed. It was not possible to image the HA gellan component due to visible cracking from evaporating/melting at low magnification in a 1% HA gellan sample. Additionally, the lack of aggregation of double helix strands means the gel structure would be very fine and therefore difficult to observe. MD gelation occurs through the formation of large crystalline regions of aggregated double helices (Chronakis, 1998). The gelation mechanism can appear as phase separated with a microscopy technique, but the lack of demixing prior to gelation excludes the applicability of phase-separated descriptions (Clark et al., 1999). TEM images of MD aggregate networks have shown microspheres of 20-30 µm (Schierbaum et al., 1984) made of smaller comb-like structures of 1-4 nm (Schierbaum et al., 1984; Clark et al., 1999; Kanyuck et al., 2019). Evidence of the smaller aggregates were seen in gels with or without HA gellan (Figure 6A and 6B). The arrangement of the microcrystalite aggregates showed differences with the presence of HA gellan, but continuous networks were observed in each. Smaller and more regular microcrystalites were observed in the mixed gel, while larger rod-like structures were formed of the aggregates for MD alone (Figure 6C and 6D). As the MD aggregated within the pores of the HA gellan network, it appears that formation of very large aggregates were prevented. This is also consistent with the images of MD with LA gellan observed by Clark et al. (1999). Although the HA gellan strands could not be seen, the modification to the MD network were consistent with an interpenetrating network.

3.2. Polymer Contributions

Compression profiles and microstructure analysis have suggested interpenetrating networks. The presence of two continuous networks naturally leads to a questioning of the specific contribution of each polymer. Utilization of the time dependence of MD aggregation allowed measurement of the direct contribution of this aggregation. The small deformation behaviour of the composite appeared most similar to the MD while the HA gellan network appeared dominant in the fracture. This was consistent with the relative magnitudes of individual properties. Composite material properties were not simply additive and showed an interaction between components during network formation. The presence of another polymer was proposed to affect the distribution and microstructure of each respective network but not the actual chemistry of the network (consistent with no changes in the enthalpy, Table 2).

Previous experiments (Figure 3) showed the concentration dependence of the composite Young's Modulus to be more strongly effected by MD than HA gellan. Considering the modulus of individual components, this was not surprising as the modulus of MD is almost a hundred times higher than that of HA gellan. It was of interest to understand the effects of MD aggregation on the composite modulus. A unique behaviour of low DE MDs is increasing gel strength, following a logarithmic function, over the time frame of weeks, (Loret et al., 2004; Kanyuck et al., 2019) and shown by in Figure 7. For gels containing MD at concentrations above (30 and 25%) and below (20, 15, and 10%) the gelation point, an increase in Young's Modulus followed a natural log function (Figure 7). HA gellan alone had the lowest Young's Modulus and was unchanged over the measured time period of 1 to 14 days. Lack of change in the HA gellan sample and the characteristic natural log curve shape suggested the increase was caused by aggregation of MD. Thus, the direct influence of MD aggregation was able to be observed. MD concentrations below the critical gelation level resulted in a modulus at an order of magnitude lower. However, both above and below the expected gelation point of MD the aggregation kinetics were the same (natural log curve shape). Aggregates of MD thus influenced the composite gel firmness even at points when a true network had not formed. As initially proposed in section 3.1.1, the aggregates added bulk and resistance to deformation. At

concentrations sufficient to form a MD gel network, MD is the major contributor to the resistance in small deformations as seen from the similarity in modulus with or without HA gellan (Figure 7 and Figure 3).

While MD aggregation caused an increase in the Young's Modulus of the composite gel, the strain and stresses at fracture exhibited behaviour more similar to HA gellan. The next experiment examined the change in fracture strain by the aggregation of MD through utilization of the time-dependence discussed previously. Concentrations of each polymer expected to form two continuous interpenetrating networks were selected for this study. The fracture of the composite is caused by breakage of the HA gellan network, while the MD is thought to modify the stress propagation (section 3.1). At the composite fracture point the MD network had already fractured. A decrease in the strain at fracture for all three concentrations of HA gellan tested corresponded to an increasingly brittle gel with aggregation of MD (Figure 8). For comparison, a 30% MD alone is also shown with fracture at a low strain (0.14 true strain). Alone a 1% HA gellan did not fracture until 0.56 true strain (Figure 2). The shifting in stain at fracture between these two extremes is proposed as an indication of inhomogeneities forming and growing in the HA gellan network by aggregation of MD. The stress at fracture was not changed ($p > 0.01$) over the 14 days (data not included). Decreasing in fracture strain was indicative of the changing distribution of HA gellan aggregates and consistent with the proposed mechanism of network heterogeneities (distribution of polymer chains and junction zone size) (Van Vliet and Walstra, 1995) and microscope images (Figure 6). As the MD aggregates grew larger, the HA gellan bends to allow the large and bulky aggregates which decreased stress propagation during compression. The influence on composite fracture also supports the proposal of MD aggregating within the pores of the HA gellan network without phase separation (IPN model). If phase separation had occurred, a continued aggregation within an excluded MD phase should not have an impact on the continuous HA gellan phase.

Due to the great difference in individual properties, each polymer was a major contributor to different composite properties. With a brittle gel and large Young's Modulus from many dense aggregates, the MD dominated the small deformation behaviour. The flexible and soft network from HA gellan dominated the fracture behaviour of the composite. Importantly, each polymer impacted the distribution (microstructure) of the other but not the chemistry of associations. The aggregation of MD made the composite stronger from the bulky aggregates and also more brittle by introducing heterogeneities into the HA gellan network.

3.3. Gelation Mechanism

The following mechanism is proposed for development of the interpenetrated networks and is illustrated in Figure 9. Initially upon cooling, HA gellan forms a network with negligible impacts from the presence of MD in solution. As the gelation is very quick, the HA gellan network has been set prior to aggregation of MD (which is consistent with DSC cooling curves). As the slow gelation of MD begins, aggregates form within pores of the HA gellan network. Growth of these regions condenses and introduces structural defects in the formerly loose and flexible HA gellan chains. Formation of these MD aggregates within the pores of HA gellan inhibits the growth of very large microcrystallites, but not the smaller helix aggregate structure. The distribution of the gellan network was also impacted by the MD, while on a chemical level the helix formations and aggregations remained unchanged (DSC confirmed the enthalpy stays the same for both polymers). Aggregates of the MD network contribute a resistance to deformation to the flexible HA gellan network. The more flexible HA gellan network was responsible for the ultimate fracture of the gel. Both polymers thus contribute to the composite physical properties and complex interactions between the networks resulted in a broad range of physical properties.

Formation of this IPN is likely caused by an associative interaction from a thermodynamic unfavourability of separation. Self-association of gellan would need to overcome the charge repulsion of the carboxylic acid groups and entropy of counterions. Concentrating similar charges into one phase is thermodynamically unfavourable and the charge repulsion theory has been proposed for other interpenetrating networks (Amici 2002). In similar cases with one ionic polymer, single phase mixtures are favoured from the higher entropy of counterions within a concentrated system (Piculell et al., 1995).The IPN suggested between MD and LA gellan supports the charge repulsion theory also occurs for the HA variant (Clark et al., 1999). It is possible that gelation of HA gellan could kinetically trap the mixed system before separation, but no indication of segregative interactions was observed in this work. Many phase separated polymers are thought to have a thermodynamic equilibrium in complete phase separation, but the gelation kinetically traps into smaller regions of separation (Kasapis et al., 1993c; Lorén et al., 1999). Future work should investigate whether segregative interactions could occur in other regimes such as controlling the gelling rates or effects of salt or pH to neutralize charge repulsion and would allow a better understanding of mechanism, but is outside the scope of this paper.

4. Conclusions:

An interpenetrating gel network of MD and HA gellan has been characterized. The mixed gel showed complex interactions between the polymers based on modification to microstructural distribution and crack propagation to fracture. Opposite textures of individual polymers have allowed an understanding of the contribution of each through analysis of the composite properties. Through microstructure modification, material properties of the composite gel shifted over a continuous range from the firm and brittle MD to the soft and flexible HA gellan. The time-influence of MD aggregation was shown to increase the modulus of the composite, but not change the fracture stress. MD aggregation showed signs of increasing brittleness through introduction of stiffness and inhomogeneities to the HA gellan network. The quick gelation and charge repulsion of HA gellan provide a thermodynamic justification for an associative interaction. The Young's Modulus, appearing almost entirely dependent on the MD contribution, supports previous claims of the limited utility of small deformation to predict texture of mixed biopolymer gels (Van den Berg et al., 2007). Small deformations and bulk fracture were needed to describe the physical properties of this IPN gel. Characterization of mixed gels from these polymers have brought a greater understanding of the physical property to microstructure relationships for multicomponent systems.

Funding. This research was partially funded by the Engineering and Physical Sciences Research Council [grant number EP/K030957/1], the EPSRC Centre for Innovative Manufacturing in Food

CRediT authorship contribution statement.

Kelsey M. Kanyuck: Conceptualization, Methodology, Formal analysis, Investigation, Writing - original draft**. Tom B. Mills:** Supervision, Writing - review & editing**. Abigail B. Norton-Welch:** Supervision, Funding acquisition, Writing - review & editing. **Ian T. Norton:** Supervision, Funding acquisition, Writing - review & editing.

References

Annable, P., M. G. Fitton, B. Harris, G. O. Phillips, & P. A. Williams. (1994). Phase behaviour and rheology of mixed polymer systems containing starch. *Food Hydrocolloids,* 8(3), 351-359.

Cassanelli, M., Norton, I., & Mills, T. (2018). Role of gellan gum microstructure in freeze drying and rehydration mechanisms. *Food Hydrocolloids,* 75, 51-61.

Chandrasekaran, R., Radha, A., & Thailambal, V. G. (1992). Roles of potassium ions, acetyl and L-glyceryl groups in native gellan double helix: an X-ray study. *Carbohydrate Research,* 224, 1-17.

Chen, B., Y. Cai, T. Liu, L. Huang, X. Zhao, M. Zhao, X. Deng, & Q. Zhao. (2020). Formation and performance of high acyl gellan hydrogel affected by the addition of physical-chemical treated insoluble soybean fiber. *Food Hydrocolloids,* 101, 105526.

Chronakis, I. S. (1998). On the molecular characteristics, compositional properties, and structural-functional mechanisms of maltodextrins: a review. *Critical Reviews in Food Science and Nutrition,* 38(7), 599-637.

Chronakis, I. S., Kasapis, S., & Richardson, R. K. (1996). Small deformation rheological properties of maltodextrin—milk protein systems. *Carbohydrate Polymers,* 29(2), 137-148.

Clark, A. H., Eyre, S., Ferdinando, D. P., & Lagarrigue, S. (1999). Interpenetrating Network Formation in Gellan− Maltodextrin Gel Composites. *Macromolecules,* 32(23), 7897-7906.

Clark, A. H. (1996). Biopolymer gels. *Current Opinion in Colloid & Interface Science,* 1(6), 712-717.

Djabourov, M., Nishinari, K., & Ross-Murphy, S. B. (2013). *Physical Gels from Biological and Synthetic Polymers*. Cambridge: Cambridge University Press.

Evageliou, V., R. K. Richardson, & E. R. Morris. (2000). Co-gelation of high methoxy pectin with oxidised starch or potato maltodextrin. *Carbohydrate Polymers,* 42(3), 233-243.

Funami, T., Noda, S., Nakauma, M., Ishihara, S., Takahashi, R., Al-Assaf, S., Ikeda, S., Nishinari, K., & Phillips, G. O. (2008). Molecular structures of gellan gum imaged with atomic force microscopy in relation to the rheological behavior in aqueous systems in the presence or absence of various cations. *Journal of Agricultural and Food Chemistry,* 56(18), 8609-8618.

Kanyuck, K. M., Mills, T. B., Norton, I. T., & Norton-Welch, A. B. (2019). Temperature influences on network formation of low DE maltodextrin gels. *Carbohydrate Polymers,*(218C), 170-178.

Kasapis, S. (2008). Phase separation in biopolymer gels: a low-to high-solid exploration of structural morphology and functionality. *Critical Reviews in Food Science and Nutrition,* 48(4), 341-359.

Kasapis, S. (1995). Review: phase separated, glassy and rubbery states of gellan gum in mixtures with food biopolymers and co-solutes. *International Journal of Food Science & Technology,* 30(6), 693-710.

Kasapis, S., Giannouli, P., Hember, M. W., Evageliou, V., Poulard, C., Tort-Bourgeois, B., & Sworn, G. (1999). Structural aspects and phase behaviour in deacylated and high acyl gellan systems. *Carbohydrate Polymers,* 38(2), 145-154.

509 Kasapis, S., Morris, E. R., Norton, I. T., & Brown, C. R. T. (1993a). Phase equilibria and gelation in
510 gelatin/maltodextrin systems - Part III: Phase separation in mixed gels. *Carbohydrate Polymers,*
511 21(4), 261-268.

512 Kasapis, S., E. R. Morris, I. T. Norton, & A. H. Clark. (1993b). Phase equilibria and gelation in
513 gelatin/maltodextrin systems — Part I: gelation of individual components. *Carbohydrate Polymers,*
514 21(4), 243-248.

515 Kasapis, S., Morris, E. R., Norton, I. T., & Gidley, M. J. (1993c). Phase equilibria and gelation in
516 gelatin/maltodextrin systems - Part II: Polymer incompatibility in solution. *Carbohydrate Polymers,*
517 21(4), 249-259.

518 Liu, L., Wang, B., Gao, Y., & Bai, T. (2013). Chitosan fibers enhanced gellan gum hydrogels with
519 superior mechanical properties and water-holding capacity. *Carbohydrate Polymers,* 97(1), 152-158.

520 Lorén, N. & Hermansson, A. (2000). Phase separation and gel formation in kinetically trapped
521 gelatin/maltodextrin gels. *International Journal of Biological Macromolecules,* 27(4), 249-262.

522 Lorén, N., Langton, M., & Hermansson, A. (1999). Confocal laser scanning microscopy and image
523 analysis of kinetically trapped phase-separated gelatin/maltodextrin gels. *Food Hydrocolloids,* 13(2),
524 185-198.

525 Loret, C., Frith, W. J., & Fryer, P. J. (2006). Mechanical and structural properties of
526 maltodextrin/agarose gel composites. *Applied Rheology,* 16(5), 248.

527 Loret, C., V. Meunier, W. J. Frith, & P. J. Fryer. (2004). Rheological characterisation of the gelation
528 behaviour of maltodextrin aqueous solutions. *Carbohydrate Polymers,* 57(2), 153-163.

529 Manoj, P., Kasapis, S., & Chronakis, I. S. (1996). Gelation and phase separation in maltodextrin-
530 caseinate systems. *Food Hydrocolloids,* 10(4), 407-420.

531 Mazen, F., Milas, M., & Rinaudo, M. (1999). Conformational transition of native and modified gellan.
532 *International Journal of Biological Macromolecules,* 26(2-3), 109-118.

533 Morris, E. R., Gothard, M., Hember, M., Manning, C. E., & Robinson, G. (1996). Conformational and
534 rheological transitions of welan, rhamsan and acylated gellan. *Carbohydrate Polymers,* 30(2-3), 165-
535 175.

536 Morris, E. R. (1995). Polysaccharide synergism—more questions than answers.In S. E. Harding, S. E.
537 Hill and J. R. Mitchell (Ed.), *Biopolymer Mixtures* (247-288). Nottingham, UK: Nottingham University
538 Press.

539 Morris, E. R. (2009). Functional interactions in gelling biopolymer mixtures.In Stefan Kasapis, Ian T.
540 Norton and Johan B. Ubbink (Ed.), *Modern biopolymer science* (167-198). : Elsevier.

541 Morris, E. R. (1992). The effect of solvent partition on the mechanical properties of biphasic
542 biopolymer gels: an approximate theoretical treatment. *Carbohydrate Polymers,* 17(1), 65-70.

543 Morris, E. R., Nishinari, K., & Rinaudo, M. (2012). Gelation of gellan–a review. *Food Hydrocolloids,*
544 28(2), 373-411.

Morris, V. J. (1986). Multicomponent gels. *Gums and Stabilisers for the Food Industry,*(3), 87-99.

Morris, V. J., Kirby, A. R., & Gunning, A. P. (1999). A fibrous model for gellan gels from atomic force microscopy studies.In K. Nishinari (Ed.), *Physical Chemistry and Industrial Application of Gellan Gum* (102-108). : Springer.

Noda, S., Funami, T., Nakauma, M., Asai, I., Takahashi, R., Al-Assaf, S., Ikeda, S., Nishinari, K., & Phillips, G. O. (2008). Molecular structures of gellan gum imaged with atomic force microscopy in relation to the rheological behavior in aqueous systems. 1. Gellan gum with various acyl contents in the presence and absence of potassium. *Food Hydrocolloids,* 22(6), 1148-1159.

Norton, A. B., Hancocks, R. D., & Grover, L. M. (2014). Poly (vinyl alcohol) modification of low acyl gellan hydrogels for applications in tissue regeneration. *Food Hydrocolloids,* 42, 373-377.

Norton, I. T. & Frith, W. J. (2001). Microstructure design in mixed biopolymer composites. *Food Hydrocolloids,* 15(4), 543-553.

Picout, D. R., Richardson, R. K., & Morris, E. R. (2000). Ca 2 -induced gelation of low-methoxy pectin in the presence of oxidised starch. Part 2. Quantitative analysis of moduli. *Carbohydrate Polymers,* 43(2), 123-131.

Piculell, L., Bergfeldt, K., & Nilsson, S. (1995). Factors determining phase behaviour of multi component polymer systems. *Biopolymer Mixtures,* 13-35.

Radosta, S. & Schierbaum, F. (1990). Polymer-Water Interaction of Maltodextrins. Part III: Non-freezable Water in Maltodextrin Solutions and Gels. *Starch-Stärke,* 42(4), 142-147.

Reuther, F., Damaschun, G., Gernat, C., Schierbaum, F., Kettlitz, B., Radosta, S., & Nothnagel, A. (1984). Molecular gelation mechanism of maltodextrins investigated by wide-angle X-ray scattering. *Colloid & Polymer Science,* 262(8), 643-647.

Ross-Murphy, S. B. (1995). Small deformation rheological behaviour of biopolymer mixtures.In S. E. Harding, S. E. Hill and J. R. Mitchell (Ed.), *Biopolymer mixtures* (85-98). Nottingham: Nottingham University Press.

Sanderson, G. R., Bell, V. L., Clark, R. C., & Ortega, D. (1988). The Texture of Gellan Gum Gels.In D. J. Wedlock & P. A. Williams (Ed.), *Gums and Stabilisers for the Food Industry 4* (219-229). Oxford: IRL.

Schierbaum, F., Kettlitz, B., Radosta, S., Reuther, F., Richter, M., & Vorwerg, W. (1984). Zum stand der kenntnisse uber struktureigenschafts-
beziehungen von maltodextrin. *Acta-Alimentaria-Polonica,* 10(69).

Schierbaum, F., Radosta, S., Vorwerg, W., Yuriev, V. P., Braudo, E. E., & German, M. L. (1992). Formation of thermally reversible maltodextrin gels as revealed by low resolution H-NMR. *Carbohydrate Polymers,* 18(3), 155-163.

Sworn, G. (2009). Gellan gum.In G. O. Phillips & P. A. Williams (Eds.), *Handbook of Hydrocolloids* (204-227). : Woodhead Publishing Limited.

Van den Berg, L., Van Vliet, T., Van der Linden, E., Van Boekel, M., & Van de Velde, F. (2007). Breakdown properties and sensory perception of whey proteins/polysaccharide mixed gels as a function of microstructure. *Food Hydrocolloids,* 21(5-6), 961-976.

Van Vliet, T. & Walstra, P. (1995). Large deformation and fracture behaviour of gels. *Faraday Discussions,* 101, 359-370.

Wang, X. & Ziegler, G. R. (2009). Phase Behavior of the ι-Carrageenan/Maltodextrin/Water System at Different Potassium Chloride Concentrations and Temperatures. *Food Biophysics,* 4(2), 119-125.

Zhang, J., Daubert, C. R., & Foegeding, E. A. (2005). Characterization of polyacrylamide gels as an elastic model for food gels. *Rheologica Acta,* 44(6), 622-630.

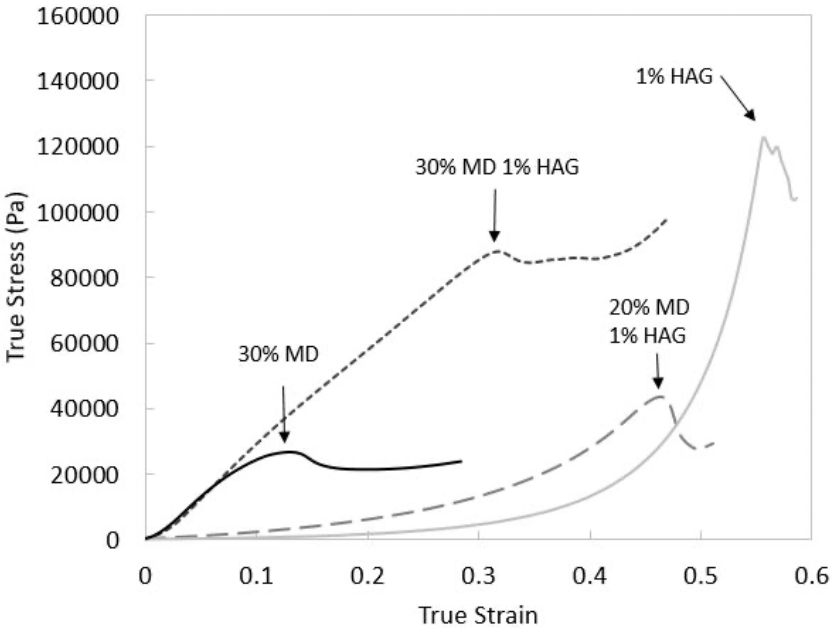

590

591 Figure 1. Compression curves for 30% MD and 1% HA gellan (HAG) (- - - -) with comparison to 30%
592 MD (—), 1% HA gellan (—), 20% MD and 1 % HA gellan (HAG) (— —) using calculated true stress and
593 true strain values. Arrows show the points of fracture for each gel.

594

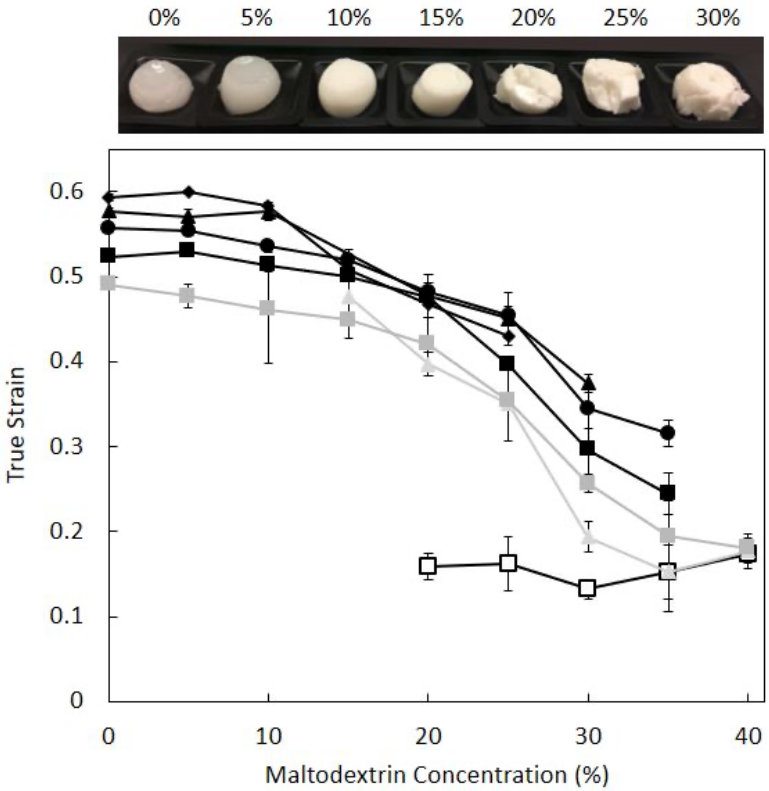

595

596 Figure 2. Comparison of the strain at failure for increasing levels of MD with HA gellan
597 concentrations of 0 % (□), 0.25% (▲), 0.5% (■), 0.75% (■), 1% (●), 1.5% (▲), and 2% (◆). Images
598 show the appearance of 1% HA gellan with maltodextrin after compression.

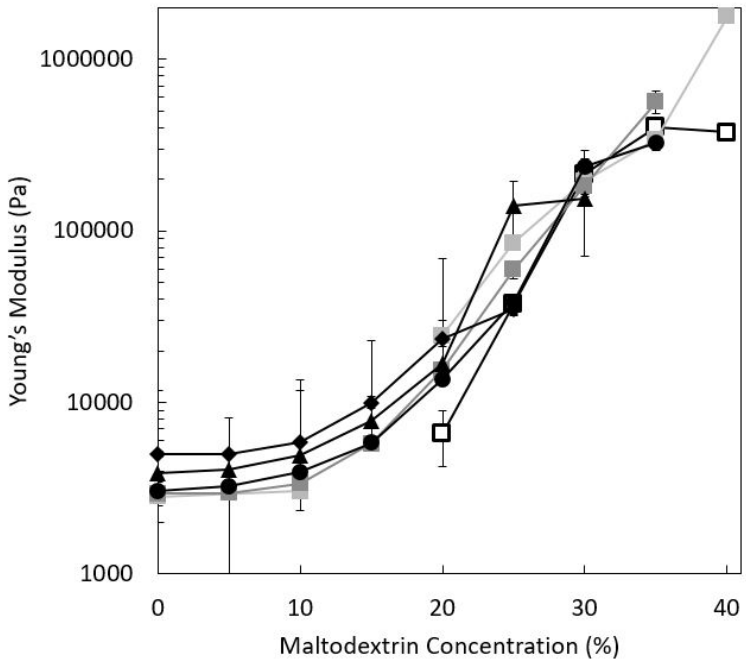

599

600 Figure 3. Small deformation mechanics before failure as indicated by the Young's Modulus for HA
601 gellan concentrations from 0 % (□), 0.25% (▲), 0.5% (■), 0.75% (■), 1% (●), 1.5% (▲), and 2% (◆) at
602 increasing levels of MD.

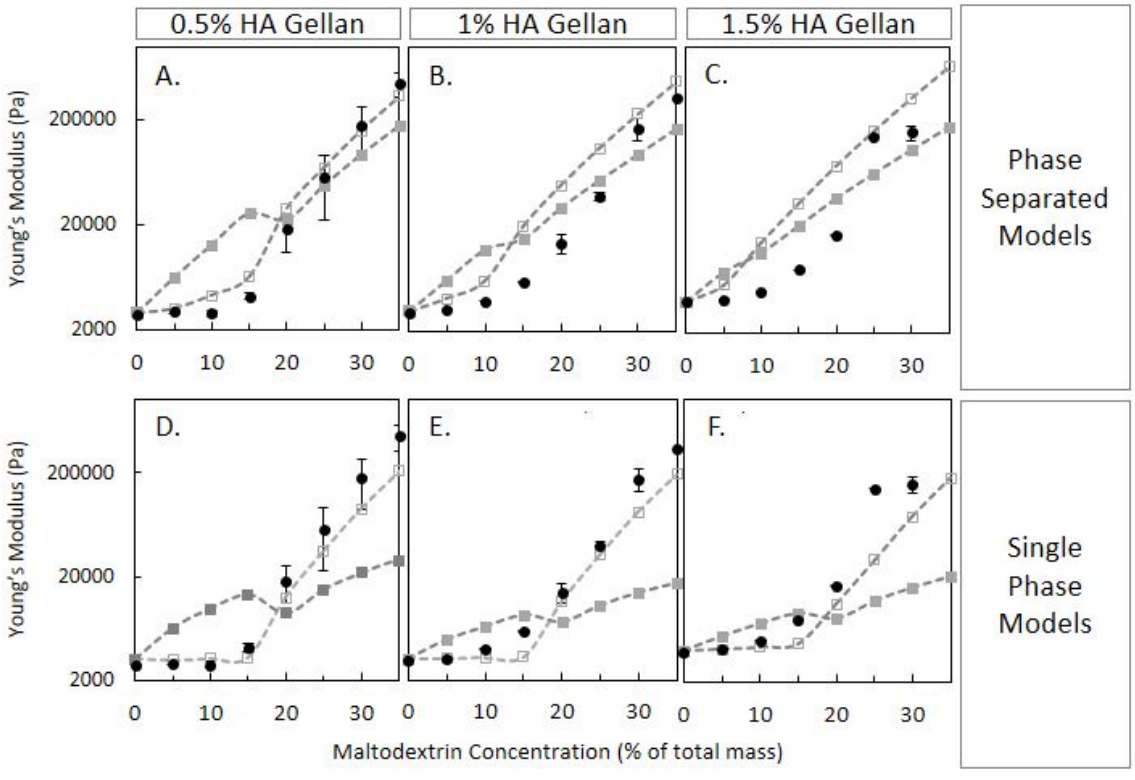

603

604 Figure 4. Comparison of measured network modulus of (A) 0.5% HA gellan, (B) 1% HA gellan and (C)
605 1.5% HA gellan with added MD (●) to calculated moduli from the isostrain (□) and isostress (■)
606 phase separation models and (D) 0.5% HA gellan, (E) 1% HA gellan and (F) 1.5% HA gellan for models
607 utilizing one phase concentrations.

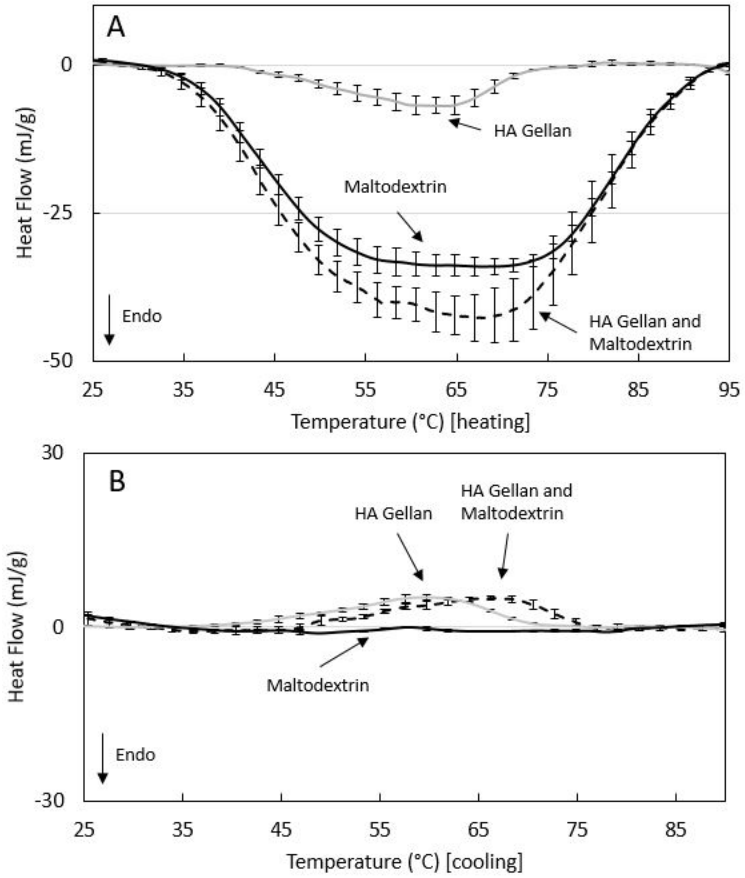

608

609 Figure 5. DSC heating (A) and cooling (B) curves for gels of 1% HA Gellan (—), 20% MD (—), and 1%
610 HA Gellan with 20% MD (- - -) after four days of gelation. After baseline subtraction, the error bars
611 represent a standard deviation of triplicate samples.

612

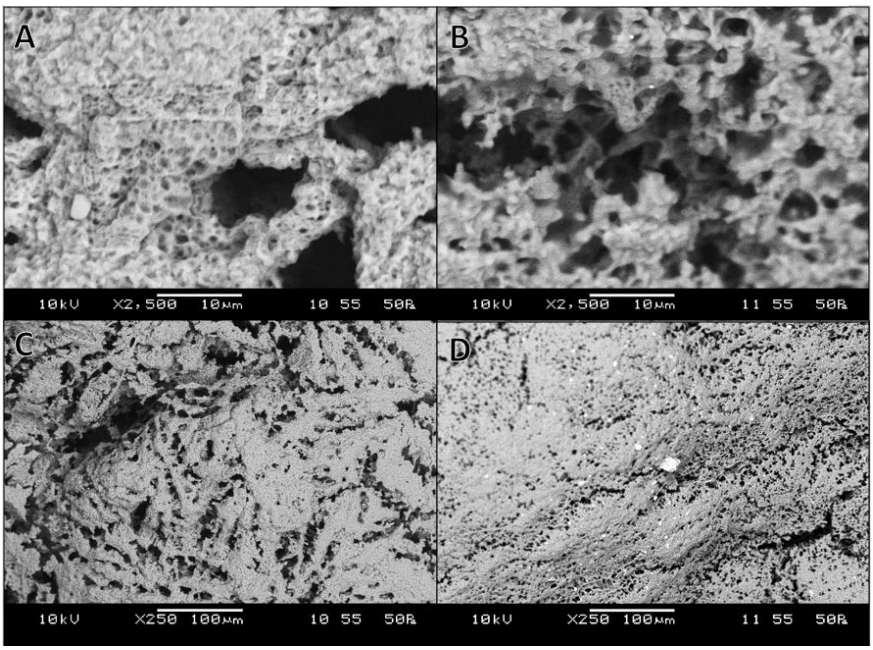

613

614 Figure 6. SEM images of 30% MD (A and C) and 1% HA gellan with 25% MD (B and D).

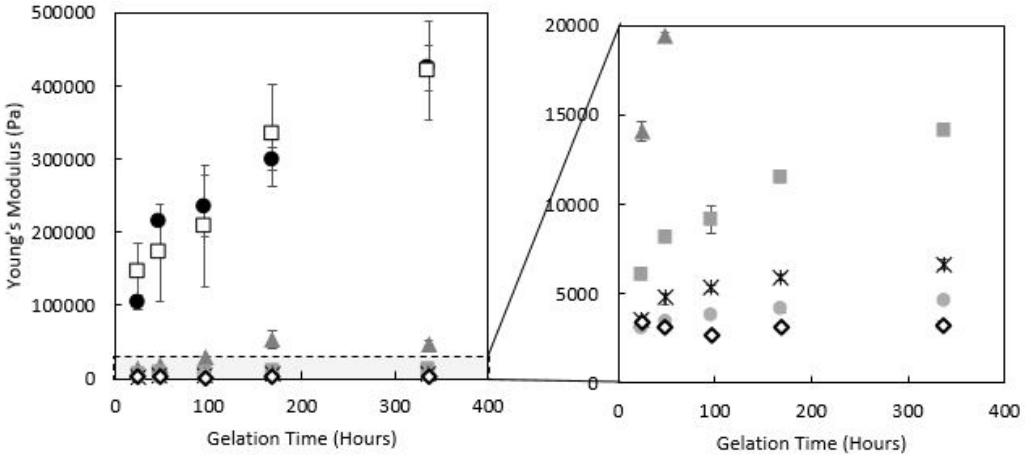

Figure 7. Contribution of MD aggregation to the composite Young's Modulus at 0 % (◇), 10% (●), 15% (X), 20% (■), 25% (▲), and of 30 % (●) to a 1% HA Gellan network and 30% MD without HA gellan (□) from 24 hours to 14 days.

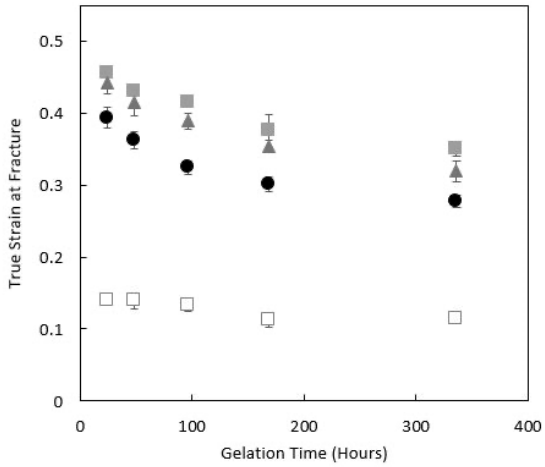

Figure 8. Contribution of MD aggregation to the true strain at fracture for mixed gels with 30% MD and 1% (●), 0.75% (■), 0.5% (▲), and 0% (□) HA gellan from 24 hours to 14 days.

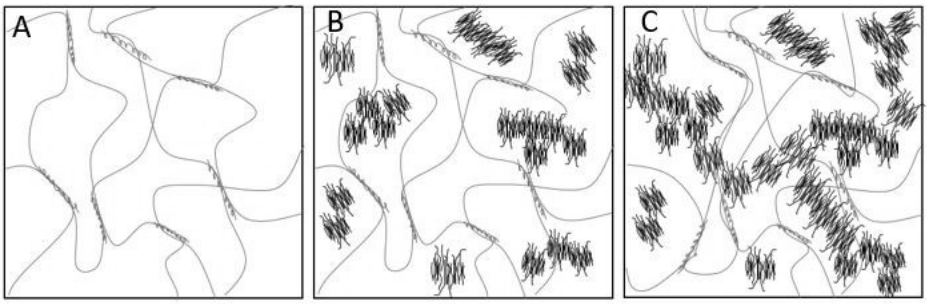

Figure 9. Proposed schematic for HA gellan network alone (A) and contributing to an interpenetrating network with MD (aggregates) below (B) and above (C) the critical gelation concentrations of MD.

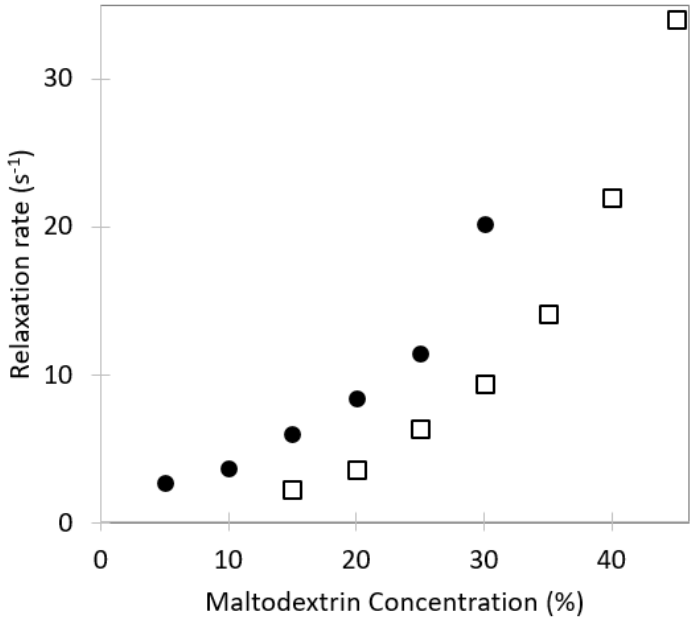

628

629 Supplementary Figure 1. NMR relaxation rates ($1/T_2$) used to estimate phase separation volumes for
630 MD (□), MD with 1% HA gellan (●). A Bruker mq20 minispec benchtop NMR was used for the
631 measurement with a CPMG pulse sequence and tau of 0.25 ms.

632

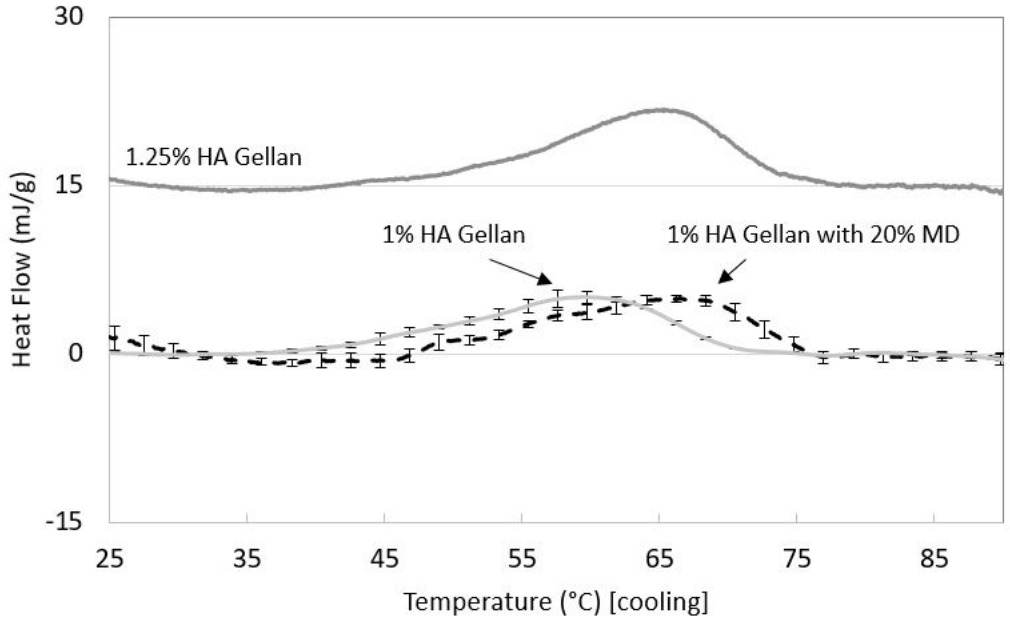

633

634 Supplementary Figure 2. DSC curves comparing melting temperature of 1% HA gellan gum with and
635 without 20% MD (from Figure 5) to 1.25% HA gellan gum.